Study of Lateral Misalignment Tolerance of a Symmetric Free-Space Optical Link for Intra International Space Station Communication

Sarah A. Tedder[1], Bryan Schoenholz[2]
NASA Glenn Research Center, Cleveland, Ohio, 44135

and

Shannon N. Suddath[3]
The University of Tulsa, Tulsa, Oklahoma, 74104

This paper describes the study of lateral misalignment tolerance of a symmetric high-rate free-space optical link (FSOL) for use between International Space Station (ISS) payload sites and the main cabin. The link will enable gigabit per second (Gbps) transmission of data, which is up to three orders of magnitude greater than the current capabilities. This application includes 10-20 meter links and requires minimum size, weight, and power (SWaP). The optical power must not present an eye hazard and must be easily integrated into the existing ISS infrastructure. On the ISS, rapid thermal changes and astronaut movement will cause flexure of the structure which will potentially misalign the free space transmit and receive optics 9 cm laterally and 0.2 degrees angularly. If this misalignment is not accounted for, a loss of the link or degradation of link performance will occur. Power measurements were collected to better understand the effect of various system design parameters on lateral misalignment tolerance. Parameters that were varied include: the type of small form-factor pluggable (SFP) optical transceivers, type of fiber, and transmitted power level. A system using 105 µm core fibers, duplex SFP's, two channels of light, and two fiber amplifiers can potentially reach the lateral misalignment tolerance (decenter span) required to create an FSOL on the ISS.

I. Introduction

The payload sites available on the International Space Station (ISS) impose significant limitations for communicating large quantities of science data due to limited bus throughput (~10 Mb/s). Physical locations of exterior payload sites impose a physical barrier to routing cables, which can be overcome by creating a wireless link. The development of high-rate free-space optical links (FSOL) for use between ISS payload sites and the main cabin (10-20 meters) will enable gigabit per second (Gbps) transmission of this data, which is up to three orders of magnitude greater than the current capabilities. The cost of delivering, installing, and operating a free-space optical link in a space environment increases with its size, weight, and power (SWaP). Our goal is to develop an eye safe, 10-20 meter reliable free-space optical link at or above 1 Gbps with minimal SWaP, which can be easily integrated into the existing ISS hardware.

On the ISS, rapid thermal changes and astronaut movement cause flexure of the structure. This flexure will misalign the free-space transmit and receive optics, potentially causing loss of the link or degradation of link performance. The flexure of the ISS is predicted to cause up to 9 cm of lateral misalignment (decenter) and 0.2 degrees of angular misalignment (tilt) over the ~25 meter distance from the ISS center of mass to the express logistics carrier payload site 3 (ELC-3)[1]. In commercially available building-to-building FSOLs,

[1]Research Aerospace Technologist, Optic and Photonics Branch, sarah.a.tedder@nasa.gov, Not a Member.
[2]Aerospace Technologist - Telecommunications, Advance High Frequency Branch, Not a Member.
[3]Graduate Assistant, Department of Electrical & Computer Engineering, Not a Member.

misalignment is solved by using amplified laser power combined with either active control or optical systems with large fields of view[2].

While active control is a proven effective solution, it increases power requirements and system complexity. This increase in requirements increases the difficultly of reducing size, weight, and power as needed by space applications. Therefore, passive solutions to misalignment in FSOL's are being studied to decrease system size and complexity, as the work in Ref. 3-8, and semi-passive work as described in Ref. 9.

Small form-factor pluggable (SFP) optical transceivers commonly used in terrestrial fiber networking links offer a high data rate with a low SWaP solution. SFPs have small detector sizes, which increase the possible data rates[8]. SFPs can also be integrated into the existing network switches on the ISS. While SFPs have many potential advantages, their small detectors decrease the tolerance to misalignment. These devices are designed to accept light from fiber optic cables with 9 µm or 62.5 µm core sizes, which have small numerical and physical apertures. These small apertures decrease the system misalignment tolerance. Hence, we investigate alternative ways to couple light into these SFPs and increase their fields of view.

This paper presents the effect of the beam divergence angle, type of SFP, fiber type, and transmitted power on the lateral misalignment tolerance (decenter span) of a 20 meter free-space optical link.

II. Experimental Setup

The following section describes the free-space optical link used to collect the data presented. The free-space optical link is setup on two optical tables placed 20 meters apart. To simulate lateral movement caused by the flexure of the ISS, the transmitter is mounted on a vertical motorized stage and the receiver is mounted on a horizontal motorized stage, as seen in Fig. 1. The modulated optical signal is created by an SFP and then, if needed, is sent to an amplifier and attenuator with single mode fibers (when not in use the amplifier and attenuator are removed from the system). Next the light is sent to the transmitter optic (a zoom collimator) using a fiber optic cable under test. The light is then collected by another identical zoom collimator and test fiber. The received light is either measured using a power meter or collected by the SFP detector depending on the measurement type.

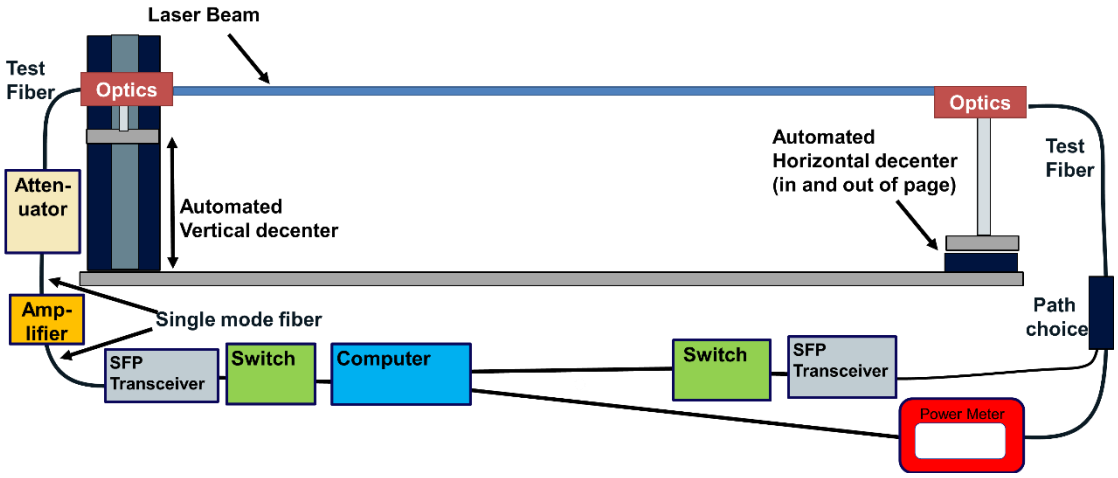

Figure 1. A sketch of the experimental setup. *The modulated optical signal is generated in a SFP and sent to the transmitter optic (a zoom collimator). The transmitter is mounted on a vertical motorized stage and the receiver is mounted on a horizontal motorized stage to simulate the flexure of the ISS. The receiver collection optics are identical to the transmitter optics. The attenuator and amplifier are optional and are removed from the system when not in use.*

A. Component Description

We investigate two types of SFP's: Duplex and single fiber bidirectional (BiDi). Duplex devices use two physically separate channels at the same wavelength (Fig. 2(a)) while single fiber BiDi devices use two different wavelengths over a single physical channel to achieve two-way data transmission (Fig. 2(b)). Both SFPs types are designed to use 1550 nm single mode fibers with LC fiber connections. We used a Catalyst

2960 plus series SI switch to power both types. The switch follows all SFP interface criterion as specified in the INF-8074i for Small Form-Factor Pluggable Transceivers[10].

We used an Optospan PSP-41DB55K080 BiDi with a transmit wavelength of 1550 nm and a receive wavelength of 1490 nm, and an Optospan PSFP-41DB49K080 which transmits 1490 nm and receives 1550 nm. Both BiDi's support a minimum data rate of 1 Gbps and a maximum of 4.25 Gbps with a detector size of 55 µm. A 45° filter is used to reflect the receive wavelength to the detector and pass the transmit wavelength as shown in Fig 2 (a). Hence, the transmit and receive signals propagate along the same path, reducing the amount of optics needed by half.

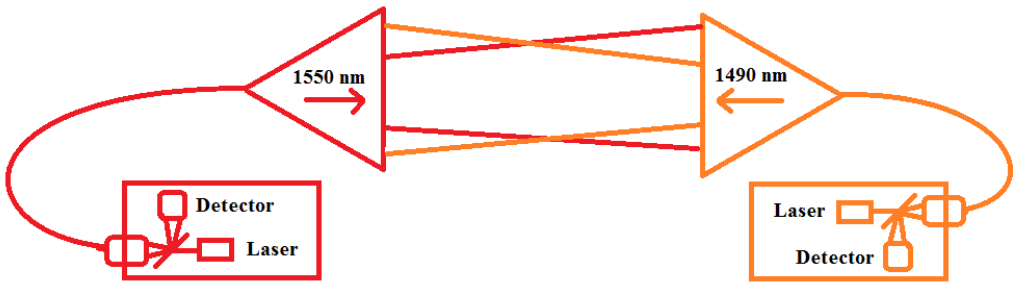

a) Link formed with Bidi SFPs

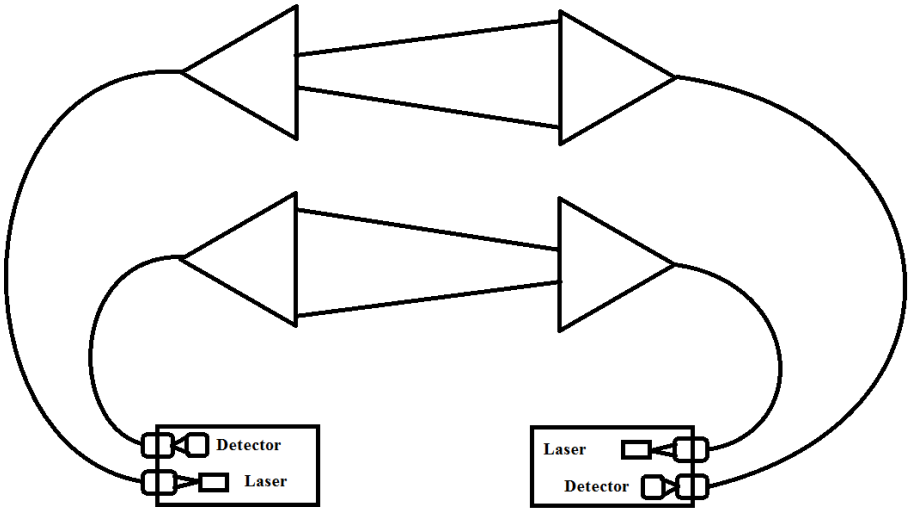

b) Link formed with Duplex SFPs

Figure 2. Sketch of SFP internals and link configurations

The Optospan PSFP-11DT55K100 Duplex transmits and receives 1550 nm and has a typical data rate of 1.25 Gbps. The Duplex SFP requires twice the amount of optics to create a symmetric link as shown in Fig 2 (b). Quoted transmit and receive limits for both types of SFPs are provided below in Table 1.

Table 1 Manufacture Quoted Transmit and Receive limits for SFPs.

SFP Type	Tx Min, dBm	Tx Max, dBm	Rx Min, dBm	Rx Max, dBm
BiDi	0	5	-24	-8
Duplex	0	5	-28	-3

A variety of test fibers is used for transmitting the light to the collimator and collecting the light on the other end of the link. Information about each fiber tested is given in Table 2 below. Each test fiber is 2 meters long and has an LC connector on the SFP side and an FC connector at the other to connect to the collimator. The first two fibers in Table 2 are standard industry fibers from L-COM used typically in terrestrial fiber networking applications where light is transmitted over large distances in fibers. The rest of the fibers are chosen to investigate misalignment qualities of the fibers in free-space applications. A single mode fiber with a large numerical aperture, Thorlabs UH4NA is selected to see the effect of increasing only the numerical aperture of the fiber. Two 50 µm fibers are chosen to assess the effect of the index of refraction transition profile from core to cladding on free-space transmitting and receiving. To study the effect of the fiber core size, the 105 µm core fiber is selected. This core size was the largest core size that could be made by the manufacturer, Thorlabs, and still be able to use the LC connection needed by the SFPs.

Table 2 Summary of Fibers Tested

Fiber	Core Size, µm	Graded Index or Step Index	Numerical Aperture (NA)
Single Mode Fiber (SMF)	10.4[a]	Graded	.12[b]
Multi-mode Fiber (MMF)	62.5	Graded	0.275
Single Mode Large Numerical Aperture (UH4NA)	9[b]	Step	0.35
Multimode Step Index Fiber (FG050LGA)	50	Step	0.22
Multimode Graded Index (GIF50C)	50	Graded	0.2
Multimode Fiber (FG105LCA)	105	Step	0.22

[a]Mode Field Diameter. [b]Not Given, Typical Reported

Thorlabs ZC618FC-C zoom collimators with FC ports are used as the transmit and receive optics. The collimators are adjustable in effective focal length and focusing distance, however for these tests, the effective focal length is set to 18 mm. To change the divergence angle the focusing distance is adjusted. The divergence angle created is calculated using a Gaussian beam approximation in Zemax. The Zemax model was created by Thorlabs and can be found on their website. The transmit and receive collimators focusing distance are always adjusted symmetrically. The collimators have an AR coating range of 1050 – 1650 nm and a maximum fiber numerical aperture of 0.25.

An Erbium-doped fiber amplifier with an operating range of 1530 – 1560 nm is used for amplification at the transmitter for some of the tests. The amplifier is placed on the transmit side in between the SFP and the zoom collimator with single mode fibers. The output power ranges from +18 dBm to +24 dBm. A digital variable attenuator is used to attenuate the amplified power. The digital variable attenuator is made for 9/125 µm single mode fibers with FC connectors and is calibrated for 1300/1550 nm. It has an accuracy of ±0.3 dB up to 40 dB attenuation. The power meter has an InGaAs photodiode fiber sensor, which has a power range of 100 pW – 3 mW and a measurement uncertainty of ±5 %.

B. Alignment Process

Since the goal is to measure the lateral misalignment tolerance, it is crucial that the link vertical and horizontal axes are perpendicular to the propagation direction. The first step in aligning the transmit and receive optics is to level each table and make sure the tables and mounted collimators are the same height

using a crosshair laser level and rulers. To level each table, a ruler is used to measure the height of the horizontal laser beam at two points on the table in both coplanar directions. Once level, a similar method is used to check and adjust the heights of the tables.

Two visible alignment lasers are used in order to align the system horizontally. Each laser is placed parallel at opposite ends of one table and is directed towards the other table. A ruler is used to measure the distance between the laser beams at each table to ensure the beams are parallel. The table without lasers is adjusted to have the parallel beams at the same relative points as the other table, and then the process is repeated by placing the lasers on the other table.

Finally, the angular alignment is performed by using infrared light and single mode fibers for transmission and collection over the experimental path. The horizontal and vertical tilts for both collimators are optimized for maximum received power at each end of the link. Angular alignment is checked in both propagation directions.

C. Data Collection

Two-dimensional power profile measurements, as shown in Fig. 3, are collected using motorized stages to decenter the transmit and receive optics. A program is used to adjust the vertical and horizontal stages in a grid around the center while reading and recording received power.

The horizontal motorized stage has a travel range of 220 mm, an absolute on-axis accuracy of ±2.0 µm, a home location accuracy of ±0.25 µm, and a minimum incremental movement of 0.1 µm. The vertical motorized stage has a travel range of 150 mm, a calibrated on-axis accuracy less than ±5.0 µm, a home location accuracy of ±0.6 µm, and a minimum achievable incremental movement of 100 nm. The typical data set used incremental movements of 2.5 or 5 mm to create the grid of data.

The minimum power required to establish a link is used as the threshold for which the decenter span is defined. Measurements of these limits are performed for many link configurations because the minimum power level to establish a link is dependent on many system factors including: SFP type, switch type, and fiber type, as shown below in section IV, Results and Discussion.

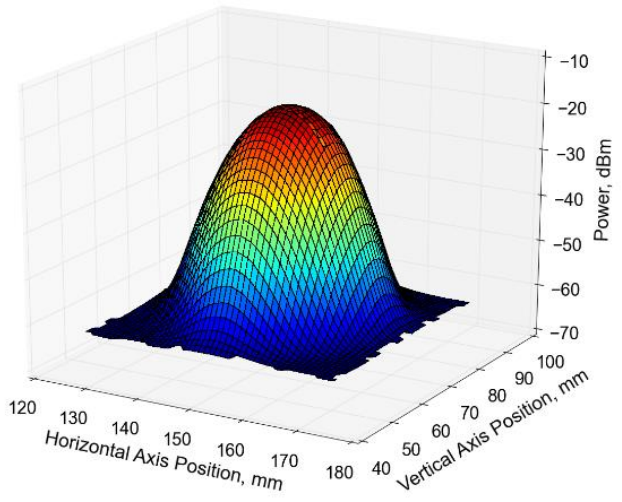

Figure 3. Sample of a 2-axis power profile. *Power profiles are collected at the receive optic of a 20 meter link by decentering the optics along 2 axes. The shown profile is measured with SMF using the Duplex SFP.*

Two types of link threshold testing were performed, fiber-only and free-space. Fiber-only tests use fibers to directly connect the SFPs over the 20 meter link, whereas fibers are only used for initial transmission and collection in free-space tests. Fiber-only tests serve as a baseline for comparison with free-space measurements. Performing these two types of measurements allow for investigation into the source of losses.

Fiber-only tests are performed by using the digital attenuator to adjust the transmitted power until the link is lost and re-established. The attenuator is added in the loop on the transmit side with single mode fibers. A 20-meter single mode fiber and the 2 m test fibers complete the SFP link.

The free-space loss of link procedure starts with aligning the system to establish a link between the SFPs. Then the vertical motorized stage is adjusted in small increments until the link is lost. Once the link is lost, the vertical stage is adjusted towards the center in small increments until the link has re-established. The received power and position is recorded and the process is repeated in the other vertical direction.

III. Data Analysis

The collected 2-axis profiles, as shown in Fig. 3, are analyzed to determine the decenter span. The decentering span is found by taking cross sections of the 2-axis profile at the maximum power location in both the horizontal and vertical directions. The distances over which the power remains above the error free receiver limit for the SFP are then identified for both the horizontal and vertical directions. The distances measured for the horizontal and vertical directions are compared and the minimum is reported as the decenter span. A baseline Zemax model of the zoom collimators created by Thorlabs is modified to match the link configuration parameters. This model is used to predict the power coupled into the receiver fiber core and beam diameter at the right before the receive collimator entrance.

IV. Results and Discussion

The following section discusses the results of power measurements collected from a 20 meter symmetrical free-space optical link. The section presents the effects of divergence angle of the transmitted beam, SFP type, fiber type, and transmitted power on the decentering span.

A theoretical model of the link with single mode fibers for the Bidi SFP predicts a ~25 % larger decenter span than was measured. The difference in the theory and model has many sources, most of which are losses from optical surface reflections train not accounted for in the theoretical model.

The repeatability of the decenter span measurement was assessed by repeating it at the same condition 5 times with SMFs. The standard deviation of the measured decenter span for the Duplex SFP was 0.1135 mm and for the Bidi SFP was 0.468 mm.

A. Optimum Divergence Angle for Maximum Decenter Span

Increasing the divergence angle produced by the transmitter increases size of the laser beam arriving at the receiver, while lowering the energy density. Figure 4 shows this effect by plotting the cross sections of the received power over a range of divergence angles. The dashed lines in the figure are the maximum and minimum receive limits defined by the SFP.

Due to these limits and the nature of how the power distribution of the light is spread, there is an optimum divergence angle at which the decenter span is maximized, as shown in Fig. 5. Figure 5 shows curves for 3 different minimum receive limits showing that the optimum divergence angle and decenter span increases with decreasing minimum receive limit. The receive limits are determined by the type of SFP. The effect of the receive limits on the decenter span are explored in section B.

The optimum divergence angle is also dependent on the magnitude and shape of the power profile received by the detector. The magnitude and shape of the received power profile is determined by the transmitting optic, the type of fiber, the transmitted power, and the receiving optic field of view. The type of fiber effect will be explored in terms of the decenter range in section C and the transmitted power is discussed in section D.

In summary, the type of SFP, fiber type, and transmitted power all effect the optimum divergence angle and therefore maximum decenter span.

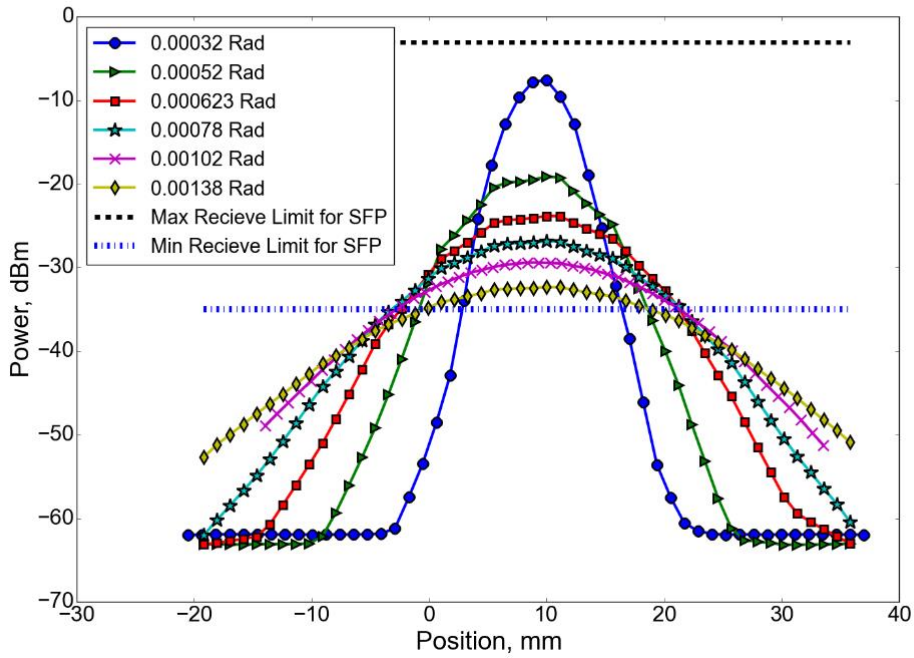

Figure 4. Power profiles for various divergence angles. *The plot shows cross sections of power profiles of received power for the configuration of SMF with the Duplex SFP. The minimum and maximum receive limits for this SFP are displayed as dashed lines.*

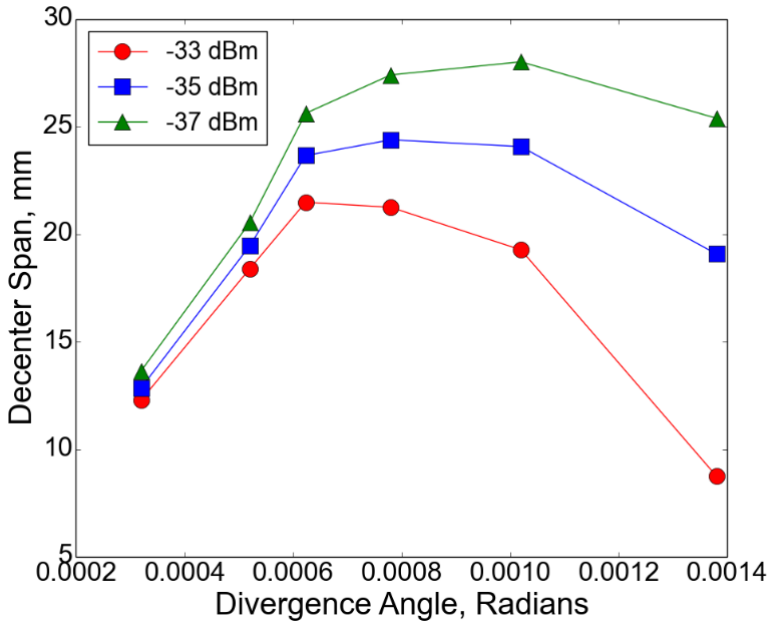

Figure 5. Effect of minimum receive limit on optimum decenter span. *This plot shows the trend of the decenter span verses the divergence angle for several minimum receive limits. Notice that as the minimum receive limit decreases the peak shifts to the left indicating an optimum divergence increase. These were measured with the SMF and Duplex SFP configuration.*

B. Type of SFP

Two different types of SFP were studied: single fiber Bidirectional (BiDi) and Duplex. The measured decentering power profile of the two types of SFPs are shown in Fig. 6. For comparison, both the SFPs were tested with SMF's, a 4.3e-4 radian optimum divergence angle, and similar transmitted powers (2.7 dBm for Bidi and 1.8 dBm for Duplex). The Duplex SFP shows a decenter power profile matching closely the BiDi SFP profile. However, the SFPs have different minimum receive limits causing a difference in the resulting decenter span potential for the SFPs.

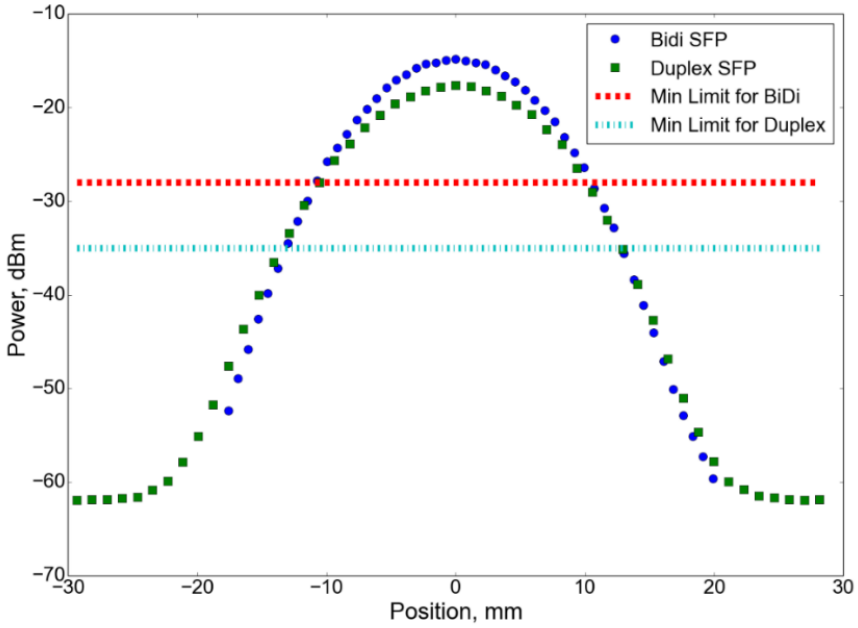

Figure 6. Comparing decenter power profiles of Duplex and BiDi SFPs. *Both profiles are taken with SMF as the transceiver fibers and a matching divergence angle of 4.3e-4 radians.*

The minimum receive limit measured for the Duplex SFP was -35.5 dBm, which is more than 7 dB lower than quoted by the manufacturer. This was measured using a fiber-only test with single mode fibers. The SFPs are designed for single mode fibers and therefore have the least amount of losses, allowing the lowest minimum receive limits.

The SMF, fiber-only measured minimum receive limits for the 1490 and the 1550 nm BiDi SFPs are -28.8 dBm and -28.2 dBm, respectively. These measured limits are about 4 dB lower than quoted for the BiDi. As seen in Fig. 6, these limits indicate a ~5 mm smaller decenter span capability for the Bidi SFP than the Duplex SFP for this system configuration.

The effect of free-space on the minimum receive limits was studied using SMF over a variety of divergence angles. The average measured minimum receive limit in free-space for the Duplex SFP is -34.9 ± 0.15 dBm. The ~0.5 dB difference between the fiber-only test and the free-space test is small enough to attribute it to errors in measurement precision. This indicates that free-space propagation using SMF for transmission and collection does not produce significant losses internally to the SFP.

For the BiDi SFPs, the minimum receive limits are affected by the difference in the index of refraction for the two transmitted wavelengths. This difference in the index produces a difference in the beam diameter at the receiver entrance. The difference between the measured 1490 nm and 1550 nm decenter spans from the power profiles is ~7 %. A Gaussian beam propagation model in Zemax verified this result, as the beam cross section at the receiver is predicted to be reduced by 7.41 % (9.8 mm to 9.1 mm). The smaller diameter of the 1490 nm beam at the receive causes the 1490 nm BiDi to reach the minimum receive limit before the 1550 nm as shown in Fig. 7. Figure 7 shows the 1550 nm power measured at the same locations that the 1490 nm reaches its receive limit at a range of divergence angles. The average minimum receive limit in free-space is -28.0 ± 0.21 dBm for the 1490 nm BiDi SFP, which is the same as the limit for the fiber-only case.

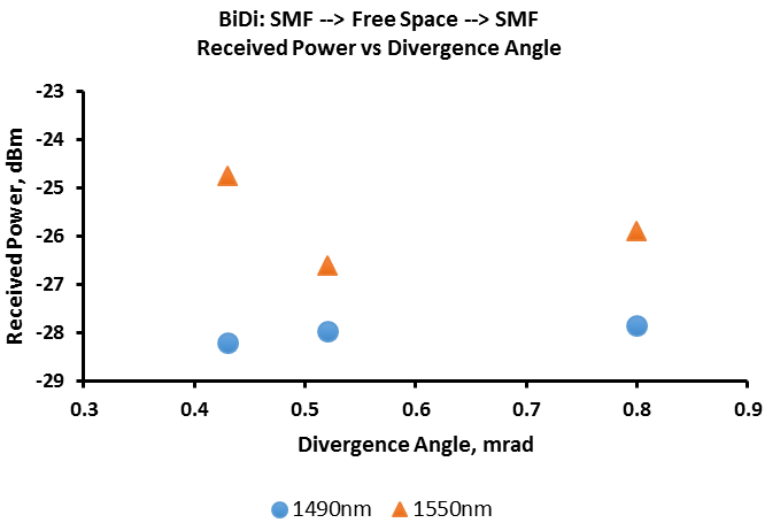

Figure 7. Minimum receive limits for BiDi SFP using SMF and propagating through free space. *Each point represents an average of two measured receive powers, one for the upper bound and one for the lower bound on the vertical decenter range. The 1550 nm points are measured at the location that the minimum receive limit is reached for the 1490 nm.*

C. Fiber Type

The effect of fiber type on the decenter span is investigated. Fiber characteristics studied include: core size, core to cladding index of refraction profile, and numerical aperture.

1. Core Size

The core size of the fiber changes the received power profile as shown in Fig. 8. The profiles shown are for their respective optimum divergence angles. The power profile transitions from a Gaussian to a top-hat profile as the core size increases.

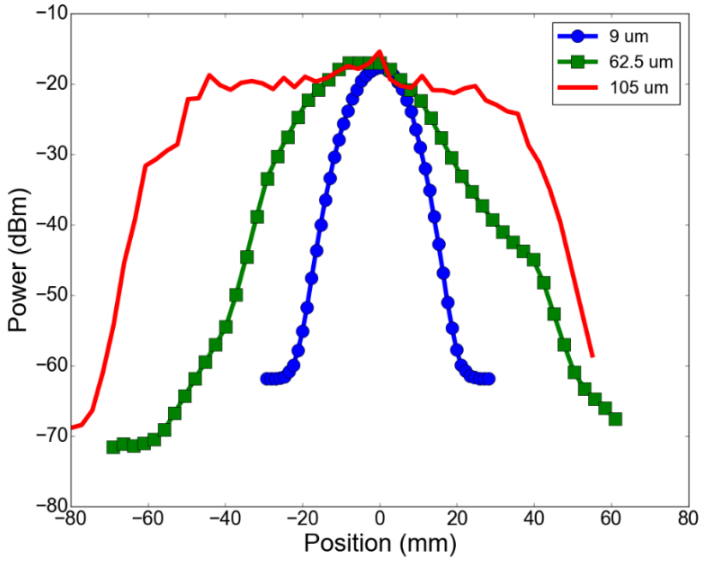

Figure 8. Cross sections of power profiles collected with various fiber core sizes. *This plots show the effect on the core size on the power profiles of received power. As the transmit/receive fiber core size increases the power distribution coverage increases.*

Figure 9 plots the decenter spans measured at optimum divergence angles verses core size. The decenter span increases with core size for both SFPs. BiDi SFPs are shown as circles and Duplex are shown as squares. The solid symbols represent the decenter span found by applying the ideal minimum receive limits (fiber-only) to the measured power profile. For this ideal case, both SFPs types coupled with the 105 µm fiber reach the decenter span goal of accommodating the ISS movement.

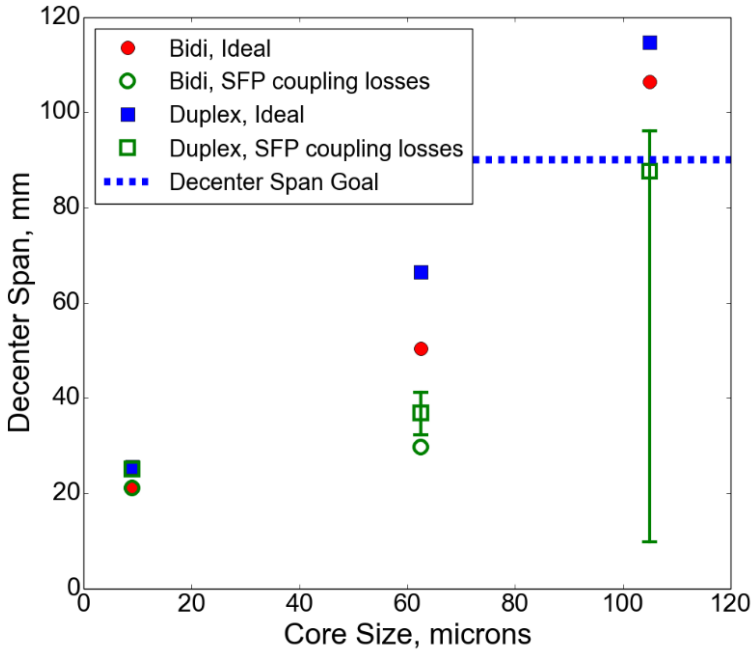

Figure 9. Core size versus decenter span. *The plot shows the core size verses the decenter span. The squares are the Duplex SFP results and the circles are the Bidi SFP results. The filled symbols show the ideal decenter spans that could be reached if no coupling losses were present. The open symbols show the actual decenter spans with the coupling losses from the SFP. The error bars represent effect of the long duration power drifts on the decenter span. Data shown is taken at optimum divergence angles.*

Unfortunately, as the core size of the fiber increases, the amount of light reaching SFP detector from the exit of the fiber core decreases. This results in an increase the minimum receive limit required to complete the link. The decenter spans resulting from the measured minimum receive limits for free-space coupling are shown with open symbols in Fig 9. The decenter spans for the 105 µm fiber with increased minimum receive limits no longer reach the goal of 9 cm. Note that there is no data point for the BiDi SFP with the 105 µm fiber because even with zero decenter of the optics the losses were too great to form a link.

We investigated the sources of these losses internal to the receiving SFP. For the MMF with the Duplex SFP, the free-space propagation minimum receive limit averaged over a range of divergence angles is -26.1 ± 1.67 dBm. This translates to 9.4 dB of losses compared to the SMF fiber only limits (lowest receive limits). The minimum receive limits measured for SMF fiber-only are compared to the 62.5 µm MMF fiber-only limits for the Duplex SFP, which accounts for 2 dB of the losses. These losses are attributed to the core diameter being larger than the 55 µm receiver at the fiber exit which increases detector overfill. The rest of the 7.4 dB of the losses indicates the free-space propagation likely causes changes in transmission at the exit of the fiber into the SFP. These changes may be due to an increase in divergence angle or from modal hits and misses on the detector.

The losses for the 105 µm fiber are even larger. The average minimum receive limit for 105 µm MMF is -25.5 ± 0.74 dBm, translating to ~10 dB in losses. The losses due to the fiber core diameter coupling to the detector is almost 4 dB higher than for the 62.5 µm multimode fiber. This is expected due to the increased core diameter causing increased detector overfill. In this case, the free-space propagation only causes ~4 dB of coupling losses internal to the SFP.

The error bars in Fig. 9 represents the possible range of decenter span that will occur over time. The maximum change in power received over 10 hours is added and subtracted from the minimum receive limit as potential losses or gain. Therefore, power levels collected in the profile are assumed to be at average power levels. The instability over time of the power increases with increase core size. The decenter span for the 105 µm fiber ranges from near 98 mm to 10 mm.

Long duration power recordings were setup to determine link power stability for various fiber core diameters. Table 3 shows the results of these tests.

Table 3. Long Duration Power Drift Test Results

Test Type	Transmit Cable Core Size, µm	Receive Cable Core Size, µm	Peak to Peak Power Swing, dBm	Standard Deviation, dBm
Free-space	9	9	0.737	0.091
Free-space	62.5	62.5	2.245	0.495
Free-space	105	105	4.475	0.733
Free-space	9	105	0.162	0.020

The stability of power over time in the link decreases as the fiber core diameter increases. To further investigate these instabilities a free-space link was setup using a 9 µm fiber at the transmitter and 105 µm fiber at the receiver. This test proved to be stable compared to the other free-space tests which indicates that the instabilities observed during testing are caused by the fiber on the transmit side of the free-space link.

2. Core to Cladding Index of Refraction Profile

Figure 10 shows power profiles of FG050LGA and GIF50C measured to compare the effect of the graded index versus the step index fiber on the decenter span. These fibers have matching core sizes but slightly different numerical apertures. They were both tested with the Duplex SFP at a matching divergence angle of 4.3e-4 radians. These measurements were made with the 50 µm fibers as the transmit and receive. The power profiles show that the step index fiber has a 25.2 % larger decenter range at the maximum potential minimum receive limit of -35 dbm. The step index profile has a flatter and more erratic top than the graded index fiber. It is important to note that while the step index fiber has advantages in decenter range, it has disadvantages in its long distance modal dispersion in the fiber.

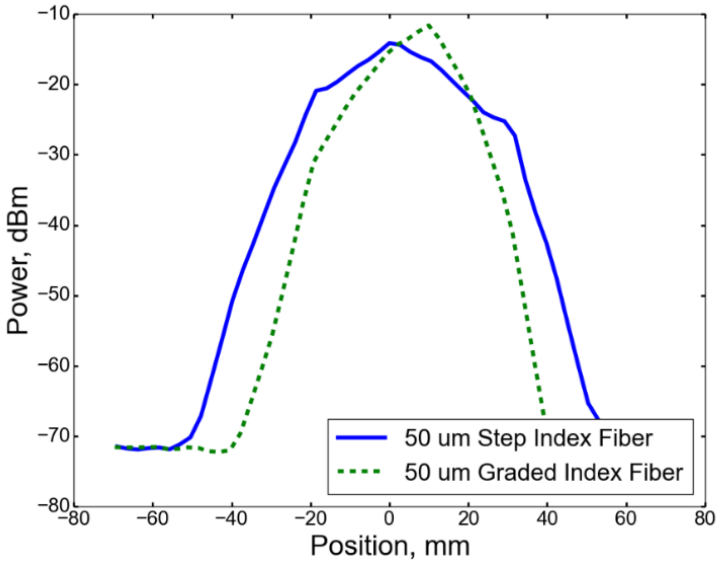

Figure 10. Received power profiles of graded index and step index fibers. *Cross sections of power profiles for 50 um core fibers one with a graded index (shown as a dashed line), one with a step index (shown as a solid line. Both are measured with the Duplex SFP and a 4.3e-4 radian divergence angle.*

3. Numerical Aperture

The effect of the numerical aperture was investigated by using two fibers with a similar core diameter but different numerical apertures as receiver fibers. The SMF has a numerical aperture near 0.12 and the UH4NA as a numerical aperture of 0.35. The power profiles are compared in Fig. 11. The UH4NA shows a lower peak power but achieves larger decenter spans for low thresholds. For the minimum receive limits of both SFPs test in this paper, the larger numerical apertures do not increase the decenter span. It is important to note the 0.35 NA of the fiber is larger than the zoom collimators (0.25). Also the SMF is a graded index fiber and the UH4NA is a step fiber so the effect seen in Fig. 11 includes the contribution of the index of refraction profile.

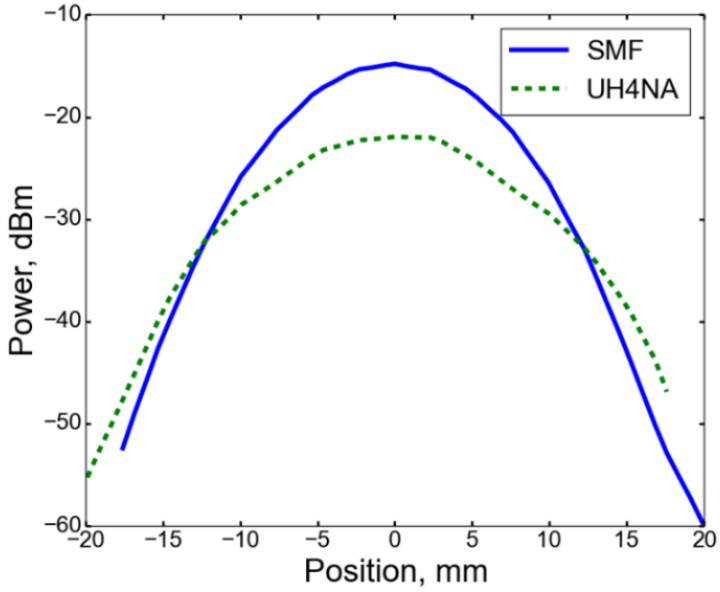

Figure 11. Received power profiles of fibers with different numerical apertures. *The plot shows cross sections of the received power profiles for single mode fibers with different numerical apertures. The index of refraction profile also is different (UH4NA is step and SMF is graded). The data was collected with a BiDi SFP and a 4.3e-4 radian divergence angle.*

D. Transmitted Power

Figure 12 shows z axis power profiles of the SMF for transmitted powers from 1.8 dBm to 9.8 dBm. The maximum power that can be sourced to the transmit optic with the entire link remaining eye safe is 9.8 dBm. Each increases of 2 dBm adds 37% more power increasing the peak height also by 37%, as expected. The decenter span on the other hand only increase 4% for each 37% increase in power when the divergence angle is kept constant. The last 37% increase in power only results in a 3% increase in decenter span.

The largest core size tested, 105 µm, shows potential to reach the decenter span goal if the coupling inside the SFP was improved. A way to overcome the losses is to increase the input power transmitted. Figure 13 shows how the decenter span increases with increasing transmitted power for the Duplex SFP. As discussed above, the received power drifts up to 4.475 dBm over time. The resulting change in decenter ranges are presented as error bars. The decenter span goal is reached with allowance for power drift at a power of 7.8 dBm. If implemented, the two sets of optics for the two channels would be required to create a symmetric link. Also, the addition of two sets of amplifiers would be needed. Both the factors add to the overall SWaP. Another possible solution to increase the transmitted power is to design custom SFPs. While the decenter span goal is reached, using the 105 µm fibers will increase the modal dispersion in the fibers. Therefore, further assessment of this solution (including Bit Error Rate measurements) are needed.

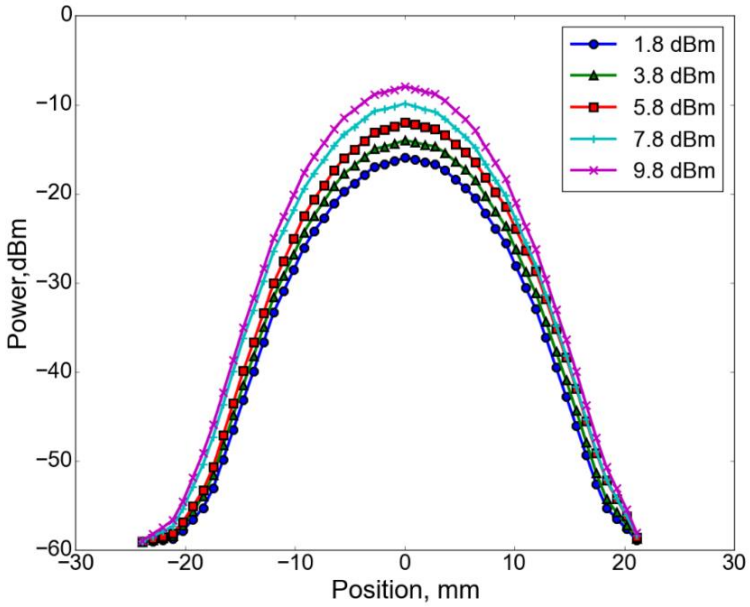

Figure 12. Cross section power profile for different transmitted powers. *Received power profiles for a range of power profiles. The peak power increases with increasing transmit power. All profiles are taken with SMF, Duplex SFP, and 4.3e-4 divergence angle.*

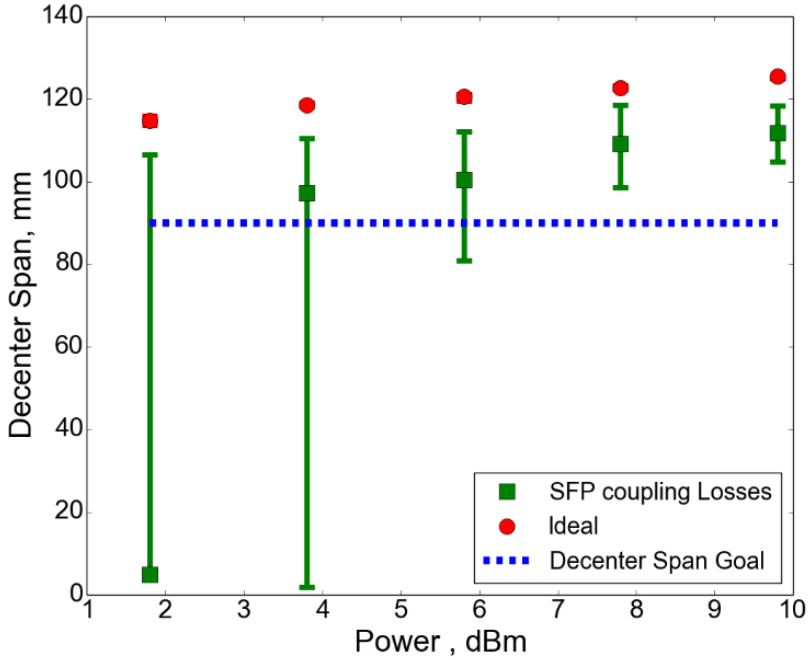

Figure 13. Power verses decenter span. *The plot shows how the decenter span varies with increasing transmitted power. The circles show the ideal decenter span if no SFP coupling losses occurred. The squares show decenter spans with the SFP coupling losses. The error bars show the potential effect of the power drift in time on the decenter span. Note that for the ideal case the error bars are so small they are barely visible on the plot. All data collected with a divergence angle of 4.3e-4.*

V. Conclusion

This paper has presented and discussed data taken to understand the effect of fiber core size, transmitted power and SFP type on the decenter span of a 20 meter symmetric FSOL. Increasing core size and power as well as using the SFP with the lowest minimum receive limit increased the decenter span. The light exiting a fiber from free-space coupling compared to fiber-only coupling produced losses internal to the SFP. The reason behind these losses will be investigated in future work.

Using 105 µm fibers, Duplex SFPs, and a pair of amplifiers creates a decenter span that can tolerate the lateral 9 cm misalignment expected on the ISS. While this configuration reaches the decenter span goal, further improvements to SWaP could be obtained with more efficient methods of coupling light into the SFP detector. Increasing the coupling efficiency to the SFP detector could eliminate the need for amplifiers or higher power custom SFPs and reduce the optics by a half. Therefore, future work will explore ways to improve the coupling. The 105µm fiber solution must also be evaluated for its bit error rate performance, as degradation to the bit error rate may occur from modal dispersion in the fiber. Future work will also include the study of angular misalignment tolerance.

Acknowledgments

This work was performed under the NASA Space Communications and Navigation (SCaN) Program for the High Data Rate Architecture Project. We want to thank Al Tucholski for building the laser tables, Sherice Sampson for moving our equipment, and Connor Nam for laboratory support.

References

[1]Schrage, D., "ISS Truss Flexure Measurement Applying Ka-Band Closed-Loop Tracking", 3rd Annual ISS Research and Development Conference, June 17- 19, 2014, Chicago.

[2]Willebrand, H. A., Ghuman, B. S., "Fiber optics without fiber," *IEEE Spectrum*, August 2001, p. 40.

[3]LoPresti, P. G., Kister, C., Spaunhorst, S., Refai, H., "Maximizing receiver misalignment tolerance in a hybrid wireless system", *Atmospheric Propagation V,* Vol. 6951, 2008.

[4]Pondelik, S., LoPresti, P. G., Refai, H., "Experimental Evaluation of a Misalignment Tolerant FSO Receiver", *Atmospheric Propagation VII,* Vol. 7685, 7685B, 2010.

[5]Jin, X., Guerrero, D., Klukas, R., Holzman, J., "Microlenses with tuned focal characteristics for optical wireless imaging", *Applied Physics Letters,* Vol. 105, No. 031102, 2014.

[6]Yun, G., Kavehrad, M., "Application of Optical Tapers to Recievers in Free Space/ Atmospheric Optical Links", In: Military Communications Conference MILCOM '90, 3:899, 1990.

[7]Bartley, T., Heim, B., Elser, D., Sych, D., Sabuncu, M., Wittmann, Lindlein, N., Marquarqt, C., Luechs, G., "Enhanced Free Space Beam Capture by Improved Optical Tapers", *Quantum Communication and Quantum Networking*, Springer Berlin, Heidelberg, 2010, Vol. 36, pp 100-107.

[8]Yun, G., Kavehrad, M., "High-angular Tolerance Receiver for Atmospheric Optical Links", *Canada Journal of Elect. & Comp. Eng.,* Vol. 16, No. 2, 1991.

[9]Brown, A. M., Hahn, D. V., Brown, D. M., Rolander, N. W., Bair, C., Sluz, J. E.," Experimental Implementation of Fiber Optic Bundle Array Wide FOV Free Space Optical Communications Receiver", *Applied Optics,* Vol. 51, No. 18, 2012.

[10]Allan, I. D., "SFP (Small Formfactor Pluggable) Transceiver", INF-8074i, Rev 1.0, May, 2001.